Iron suppresses erythropoietin expression via oxidative stress-dependent hypoxia-inducible factor-2 alpha inactivation

Keisuke Oshima[1,2*], Yasumasa Ikeda[1*], Yuya Horinouchi[1], Hiroaki Watanabe[3], Hirofumi Hamano[1,4], Yoshitaka Kihira[1,5], Seiji Kishi[6], Yuki Izawa-Ishizawa[1], Licht Miyamoto[7], Tasuku Hirayama[8], Hideko Nagasawa[8], Keisuke Ishizawa[3,6], Koichiro Tsuchiya[7], Toshiaki Tamaki[1]

[1]Department of Pharmacology, Institute of Biomedical Sciences, Tokushima University Graduate School, Tokushima, Japan

[2]Student Lab, Tokushima University Faculty of Medicine

[3]Department of Clinical Pharmacy, Institute of Biomedical Sciences, Tokushima University Graduate School, Tokushima, Japan

[4]Department of Pharmacy, Tokushima University Hospital, Tokushima, Japan

[5]Department of Clinical Pharmacy, Faculty of Pharmacy and Pharmaceutical Sciences, Fukuyama University, Fukuyama, Japan

[6]Department of Nephrology, Institute of Biomedical Sciences, Tokushima University Graduate School, Tokushima, Japan

[7]Department of Medical Pharmacology, Institute of Biomedical Sciences, Tokushima University Graduate School, Tokushima, Japan

[8]Laboratory of Pharmaceutical and Medicinal Chemistry, Gifu Pharmaceutical

University

*These authors equally contributed to this work.

Running title: Inhibitory action of iron on erythropoietin via oxidative stress-HIF-2α pathway

Name and postal and email addresses for the corresponding author:

Yasumasa Ikeda

Associate Professor, Department of Pharmacology, Institute of Biomedical Sciences, Tokushima University Graduate School

3-18-15 Kuramoto-cho, Tokushima, 770-8503, Japan

E-mail: yasuike@tokushima-u.ac.jp

Phone: +81-88-633-7061; Fax: +81-88-633-7062

Abstract

Renal anemia is a major complication in chronic kidney disease (CKD). Iron supplementation, as well as erythropoiesis-stimulating agents, are widely used for treatment of renal anemia. However, excess iron causes oxidative stress via the Fenton reaction, and iron supplementation might damage remnant renal function including erythropoietin (EPO) production in CKD. *EPO* gene expression was suppressed in mice following direct iron treatment. Hypoxia-inducible factor-2 alpha (HIF-2α), a positive regulator of the *EPO* gene, was also diminished in the kidney of mice following iron treatment. Anemia-induced increase in EPO and HIF-2α expression was also inhibited by iron-treatment. In *in vitro* experiments using EPO-producing HepG2 cells, iron stimulation reduced the expression of the *EPO* gene, as well as *HIF-2α*. Moreover, iron treatment augmented oxidative stress, and iron-induced reduction of *EPO* and *HIF-2α* expression was restored by tempol, an anti-oxidant compound. HIF-2α interaction with the *EPO* promoter was inhibited by iron treatment, and was restored by tempol. These findings suggested that iron supplementation reduced *EPO* gene expression via an oxidative stress-HIF-2α-dependent signaling pathway.

Introduction

The incidence of chronic kidney disease (CKD) has increased worldwide, and CKD worsens morbidity and mortality in the general population[1, 2]. Additionally, the progression of CKD results in end-stage renal failure, which requires treatment by hemodialysis or renal transplantation. In addition, a variety of complications arises during the course of CKD. Cardiovascular disease, a major complication of CKD, also leads to worse outcomes in CKD patients[3]. Renal anemia is commonly seen in individuals with CKD due to insufficient erythropoietin (EPO) production within the diseased kidney[4, 5]. Therefore, patients with end stage renal disease receive erythropoiesis-stimulating agent (ESA) for treatment of renal anemia.

Iron supplementation, in addition to ESA, is often used for treatment of renal anemia [6]. However, patients with CKD often show functional iron deficiency, rather than absolute iron deficiency, characterized by impaired iron release from body iron stores [7]. Disturbance of iron utilization in CKD occurs due to ferroportin (an cellular iron exporter) degradation resulting from increased hepcidin production[8, 9]. Hepcidin is a positively controlled by iron stores[10]. Therefore, iron treatment further exacerbates impaired iron utilization via hepcidin elevation and result in over accumulation of disused iron in organs of CKD individuals. Actually, adverse effects of iron supplementation on organs have been directly observed in several studies. Iron sucrose treatment exacerbates endothelial dysfunction in healthy subjects[11] and atherosclerotic change through enhancement of oxidative stress in a CKD mouse model[12]. Intravenous

iron also causes oxidative stress and transient proteinuria, tubular damage and inflammatory cytokine production in patients with CKD[13, 14]. Thus, parenteral iron supplementation might aggravate and cause complications in CKD through oxidative stress production. Furthermore, iron might exacerbate erythropoietin production consequent to remnant kidney injury, however, the effect of iron on EPO regulation has not been elucidated.

Here, we demonstrate that saccharated ferric oxide (SFO) reduced renal *EPO* expression through iron-induced oxidative stress production dependent inactivation of hypoxia-inducible factor-2α. Our findings suggest that therapeutic iron supplementation has a harmful effect on *EPO* regulation in remnant kidney function, causing a vicious cycle of CKD progression.

Materials and Methods

Materials

We purchased saccharated ferric oxide (SFO), cobalt chloride ($CoCl_2$), tempol, and dimethyloxallyl glycine (DMOG) from Nichi-Iko Pharmaceutical Co., Ltd (Toyama, Japan), Wako Pure Chemical Industries, Ltd. (Osaka, Japan), Sigma-Aldrich (St. Louis, MO, USA), and Cayman Chemical Company (Michigan, USA), respectively. The following commercially available antibodies were used: anti-HIF-2α (R&D Systems, Inc. Minneapolis, MN, USA); anti-HIF-1α (Cayman Chemical Company, Ann Arbor, MI, USA); anti-PDGF-Rβ (Cell Signaling Technology, Beverly, MA, USA); anti-α-SMA (Sigma-Aldrich, St. Louis, MO, USA); anti-Lotus

Tetragonolobus Lectin (VECTOR Laboratories, Burlingame, CA, USA); E-cadherin (Cell Signaling Technology Japan, K.K., Tokyo, Japan); anti-α-tubulin, as a loading control, from Calbiochem (San Diego, CA, USA).

Animal preparation and procedure

All experimental procedures were performed in accordance with the guidelines of the Animal Research Committee of Tokushima University Graduate School, and protocols were approved by the Institutional Review Board for animal protection. Eight-week-old C57/BL6J mice were obtained from Nippon CLEA (Tokyo, Japan) and they were maintained with free access to water and food (Type NMF; Oriental Yeast, Tokyo, Japan). The unilateral ureteral obstruction (UUO) procedure was previously described in detail[15]. Our mouse model of chronic iron treatment was produced as previously described[12]. Briefly, intraperitoneal SFO (2 mg in a volume of 200 μl) ·25 g mouse^{-1}) or the same volume of vehicle was administered for five consecutive days. Mice were sacrificed 24 h after the last iron treatment. Mice were killed with an intraperitoneal injection of over-dose pentobarbital, and the kidney was removed and stored at −80°C until use.

Induction of anemia by phlebotomy

Phlebotomy was performed for two consecutive days. Briefly, after anesthesia, approximately 400 μL blood was removed via retroorbital bleeding and was replaced by the same volume of sterile normal saline by a subcutaneous injection. Then, mice were administered the vehicle or SFO via an intraperitoneal injection and were placed

on a heating pad until full recovery. Mice were sacrificed 24 h after the last phlebotomy.

Cell culture

Although renal EPO-producing cells are suggested to be derived from tubular interstitial cells such as fibroblasts [16, 17] or pericytes[18], there are no cell lines established. Therefore, HepG2 cells, a human hepatoma cell line, have been used as EPO-producing cells in *in vitro* experiments [19-21]. Similarly, we used HepG2 cells to investigate the mechanism of iron on EPO regulation in this study. HepG2 cell was purchased from the Japanese Collection of Research Bioresources (Osaka, Japan). Cells were cultured in Dulbecco's Modified Eagle's Medium (DMEM) **(**Wako Pure Chemical Industries, Ltd., Osaka, Japan) according to the protocol. For each experiment, cells at passage 5–8 were used. Cells were grown to confluence then transferred to serum-free medium before the start of the experiments. In some experiments, cells were pretreated with 100 μM $CoCl_2$, 200 μM DMOG, and 100 μM tempol for 1 h before stimulation with SFO.

RNA extraction and evaluation of mRNA expression levels

RNA extraction, cDNA synthesis, and quantitative RT-PCR methods have been previously described[15]. Briefly, tissues or cells were homogenized in RNAiso reagent (TAKARA Bio, Inc., Otsu, Japan). RNA extraction and cDNA synthesis were performed according to the manufacturer's instructions (PrimeScript RT reagent Kit with gDNA Eraser (Perfect Real Time), TAKARA Bio, Inc.). Quantitative RT-PCR

was performed using the CFX Connect Real-Time PCR Detection System (BIO-RAD Laboratories Inc., Hercules, CA, USA) with THUNDERBIRD SYBR qPCR Mix (TOYOBO CO., LTD., Osaka, Japan). The expression levels of all target genes were normalized using *36B4* as an internal control[15]. The primer sets used are noted in Table 1.

Protein extraction and western blot analysis

Protein preparation and western blotting were performed as previously described[15]. Briefly, the tissues or cell samples were homogenized and sonicated, and then proteins were extracted. Extracted proteins were boiled for 5 min in Laemmli sample buffer and separated using SDS-PAGE. Proteins were transferred to a polyvinylidene fluoride (PVDF) membrane and the membrane was blocked for 1 h at room temperature. Next, the membrane was incubated individually with each primary antibody overnight at 4°C, followed by incubation for 1 h with the secondary antibody. Immunoreactive bands were detected using a chemiluminescence reagent and visualized by exposure onto an X-ray film or by C-DiGit chemiluminescent scanner (LI–COR C-DiGit Blot Scanner, Lincoln, Nebraska, USA). Densitometry of the visualized bands was quantified using Image J 1.38x software.

Immunohistochemistry in the kidney

Extracted kidney tissues were embedded in OCT compound (Tissue-Tek, SAKURA Finetek, Tokyo, Japan) and frozen in liquid nitrogen-cold isopentane. Samples were cut into 8-μm sections, dried, and fixed in 4% paraformaldehyde for 10

min. After blocking, the tissue sections were incubated with 1:100 dilution of primary antibody at 4°C overnight. Antibody distribution was visualized using immunofluorescence (Alexa fluor; Life Technology, Tokyo, Japan). Sections incubated without primary antibody were used as negative controls.

Measurement of tissue iron content

Tissue iron content was measured using an iron assay kit according to the manufacturer's instructions (Metallo assay, Metallogenics Co., Ltd., Chiba, Japan) as described previously[15, 22]. Briefly, extracted kidney tissues were weighed and homogenized in cell lysis buffer. Non-centrifuged crude lysates were additionally sonicated, then added and mixed with 6 N hydrochloric acid to a final concentration of 0.05 M at room temperature for 30 min. After centrifugation, supernatants were used for iron measurement. Tissue iron concentration was corrected using tissue weight and expressed as μg $Fe \cdot g^{-1}$ wet tissue.

Cell viability assay

Cell viability was accessed using CellTiter 96 AQueous nonradioactive cell proliferation assay kit (Promega KK, Tokyo, Japan)[23]. Briefly, HepG2 cells were seeded in 96-well plates at 1×10^4 cells per well and incubated for 24 h. Subsequently, various concentrations of SFO were added for 24 h and the impact of SFO on cell viability was assessed 1 h after the addition of MTS reagent by measuring absorbance

at 490 nm with a plate reader (iMARK microplate reader, BIO-RAD Laboratories Inc., Hercules, CA, USA).

Detection of labile ferrous iron

We used RhoNox-1 to detect intracellular labile ferrous iron. RhoNox-1 was kindly provided from Dr. Tasuku Hirayama and Prof. Hideko Nagasawa [24]. In brief, an unfixed frozen section of the kidney was washed with Hank's Balanced Salt Solution (HBSS) 3 times and incubated with RhoNox-1 in HBSS (5 μM) in a dark, humidified container at room temperature for 30 min. After washing with HBSS 3 times, section was covered with a small drop of the mounting medium, and observed using fluorescence microscopy. In some experiments, frozen sections were fixed in 10% neutral formaldehyde for 1 min, washed with HBSS, and incubated with RhoNOX-1[25]. Then, the sections were incubated with the primary antibody at 4°C overnight in a dark humidified container. Lectin or E-cadherin was used as a marker of the proximal or distal tubules, respectively. In HepG2 cells, cells were seeded in a 24-well culture plate or a black 96-well microplate. HepG2 was stimulated with SFO for 1 h and then loaded with 5 μM RhoNox-1 in HBSS at 37°C for 30 min. After washing, ferrous iron was observed using fluorescence microscopy or quantitatively measured at 530 and 575 nm for RhoNox-1 using a fluorescence microplate reader (Varilskan Flash, Thermo Fisher Scientific, Waltham, MA, USA).

In situ oxidative stress detection in kidney tissue

Detection of superoxide production in the kidney was evaluated by dihydroethidium (DHE) staining method as described previously[22]. Briefly, non-fixed frozen tissue sections were incubated with DHE in PBS (10 μM) in a dark, humidified container at room temperature for 30 min and then observed using fluorescence microscopy.

Intracellular reactive oxidative species detection

Intracellular reactive oxidative species (ROS) were detected using 2′,7′-Dichlorofluorescin diacetate (DCFH-DA) (Sigma-Aldrich, St. Louis, MO, USA). HepG2 was stimulated with SFO for 1h and then loaded with 10 μM DCFH-DA at 37°C for 30 min. After washing, ROS production was observed using fluorescence microscopy or quantitatively measured at 488 and 532 nm for DCFH-DA using a microplate reader (FilterMax F3 Multi-Mode Microplate Readers, Molecular Devices, LLC., Sunnyvale, CA, USA).

Chromatin immunoprecipitation

Chromatin immunoprecipitation (ChIP) was performed to determine the interaction between the hypoxia-inducible factor-2 alpha HIF-2α protein and *Epo*-gene promoter containing the hypoxia response element (HRE). Briefly, HepG2 cells treated with vehicle or SFO, and with or without tempol were crosslinked with formaldehyde at final concentration of 1.0% for 10 min, then added to 2.5 mM glycine to stop the crosslinking reaction. Then, cells were collected, incubated with cell lysis buffer, and

the nuclear fraction was extracted. After sonication and centrifugation, the supernatant fraction was co-immunoprecipitated with HIF-2α protein using agarose beads (Protein A/G plus-Agarose, Santa Cruz Biotechnology, Inc.). The beads were washed and incubated at 65°C in elution buffer to reverse the cross-links. DNA was purified from the elution buffer and used for PCR. The primer sequence for the HRE-containing region of the human EPO promoter was used as shown previously[26]. The primer sequences, used to amplify the HRE-containing region of the human *EPO* promoter were as follows: *EPO* forward primer 5'- TCGTTTTCTGGGAACCTCCA-3', and *EPO* reverse primer 5'-GGAGC- CACCTTATTGACCAG-3'.

Hypoxia-responsive element Luciferase Reporter Assay

The hypoxia-responsive reporter vector was constructed using 3 tandem copies of the hypoxia-responsive element (HRE) from the human EPO gene subcloned into the secreted luciferase from the marine copepod *Metridia longa* transcription unit (pCre-MetLuc2-Reporter plasmid vector, Takara Bio Inc. Shiga, Japan). One-hundred ng pCre-MetLuc-HRE plasmid vector and 10 ng pSEAP2-Control plasmid vector (Takara Bio Inc.) were co-transfected in 1×10^4 HepG2 cells using Lipofectamine 2000 (Thermo Fisher Scientific Inc.) in a 96-well culture plate. The transfected cells were exposed to the vehicle or SFO for 24 h and then the cell culture medium was harvested and both luciferase and alkaline phosphatase (ALP) activities were measured using Secreted Luciferase Reporter Assay (Takara Bio Inc.) and SEAP Reporter Gene

Assay (Sigma-Aldrich Japan K.K., Tokyo, Japan), respectively, according to the manufacturer's instructions. To normalize the transfection efficiency, the RLU of the luciferase chemiluminescence unit was divided by that of the ALP chemiluminescence unit.

Measurement of plasma EPO concentration

Plasma EPO concentration was determined by using an ELISA kit, according to the manufacturer's instructions (Mouse Erythropoietin Quantikine ELISA Kit, R&D systems Inc., Minneapolis, MN, USA).

Statistical analysis

Data are presented as mean ± standard deviation (SD). An unpaired, 2-tailed Student's *t*-test was used for comparison between the two groups. For comparisons between more than two groups, the statistical significance of each difference was evaluated by post-hoc test using Dunnett's method or Tukey-Kramer's method. Statistical significance was indicated by $P < 0.05$.

Results

EPO expression and iron content in the kidney with UUO surgery

EPO mRNA levels are drastically reduced in kidneys with UUO surgery[17]. Similarly, EPO mRNA expression was decreased in the kidney at 7 days after UUO surgery compared to sham-operation (Figure 1A). We have already demonstrated that

renal iron content was significantly augmented in UUO-induced fibrotic kidney in the previous study [15].

EPO expression and iron content in the kidney of iron-treated mice

To examine direct action of iron on EPO expression, we used mice with SFO treatment. Renal iron content was significantly increased in mice with SFO treatment for consecutive five days compared to vehicle-treated mice (vehicle; 12.0 ± 3.6 μg $Fe \cdot g^{-1}$ wet tissue, SFO; 20.8 ± 4.2 μg $Fe \cdot g^{-1}$ wet tissue, n=3, $p<0.05$). *EPO* mRNA expression was decreased in the kidney of SFO-treated mice compared to vehicle-treated mice (Figure 1D). Similarly, the plasma EPO concentration was also suppressed in SFO-treated mice (Table 4). There were no significant differences in hematological parameters of red blood cells between vehicle- and SFO-treated mice (Table 2).

HIF-2α *expression in the kidney with UUO and iron-treated mice*

HIF-2α is an important regulator of *EPO* expression in the kidney[27] and liver[26]. HIF-2α expression was diminished in the kidneys with UUO and iron treatment compared to the kidneys with sham- or vehicle-treatment (Figure 1C and F). These findings suggest that iron accumulation suppresses renal *EPO* expression through the inhibition of HIF-2α. In contrast, HIF-1α mRNA was not changed and HIF-1α protein was decreased in the kidney of UUO mice (Figure 1B and C), whereas HIF-1α mRNA

was elevated and HIF-1α protein tended to decrease in the kidney of SFO-treated mice (Figure 1E and F).

SFO action on transition of fibroblast to myofibroblast in kidneys

EPO production occurs in fibroblasts, and loss of *EPO* production occurs during the transition of fibroblast to myofibroblast in the course of renal fibrosis progression[16, 17]. The fibroblast to myofibroblast transition plays an important role in the process of renal fibrosis[28]. Therefore, we checked whether iron was involved in the fibroblast to myofibroblast transition-dependent loss of *EPO* production. No apparent parenchymal damages were seen in the kidney of SFO-treated mice compared to vehicle-treated mice (Figure 2A). SFO treatment augmented the expression of PDGF-Rβ and α-SMA proteins in the kidney, compared to vehicle treatment (Figure 2B and C). Immunohistochemical analysis showed that PDGF-Rβ expression was increased in the renal interstitium of SFO-treated kidneys. α-SMA expression also increased in the renal interstitium of SFO-treated kidneys. In contrast, it was almost completely localized in vessels in vehicle-treated kidneys. Moreover, PDGF-Rβ and α-SMA expression were colocalized in the renal interstitium of SFO-treated kidneys (Figure 2D). These results suggest that iron-induced EPO reduction occurs due to an induction of renal fibrotic change and the myofibroblast transition.

The effect of SFO on EPO mRNA expression in HepG2 cells

First, we performed the MTS cell proliferation assay to determine the effect of SFO on the viability of HepG2 cells. SFO had no effect of cellular viability at 50, 100, and 200 $\mu g \cdot ml^{-1}$ but significantly reduced cell viability at 1000 $\mu g \cdot ml^{-1}$. This result indicates that high concentrations of SFO are toxic for HepG2 cells (Figure 3A). Therefore, we used SFO at concentrations of 200 μg/ml and below in further studies. To examine the effect of SFO on *EPO* mRNA expression, we examined *EPO* mRNA expression after treatment with various concentration of SFO. As shown in Figure 3B, SFO significantly reduced *EPO* mRNA expression in a dose-dependent manner. HIF-2α mRNA and protein levels were also reduced by SFO treatment in HepG2 cells (Figure 3C and D). In contrast, the expression of HIF-1α at the mRNA and protein levels decreased in HepG2 cells (Figure 3C and D). The results of these *in vitro* experiments are consistent with i*n vivo* results demonstrating the effect of SFO on *EPO* and *HIF-2α* expression in the kidney.

The suppressive effects of SFO on $CoCl_2$ or DMOG-induced EPO and HIF-2α upregulation

We examined the effects of SFO on *EPO* and HIF-2α expression under hypoxic conditions, using cobalt chloride to mimic conditions of hypoxia induction. *EPO* mRNA and HIF-2α protein expression were increased by cobalt chloride treatment. The hypoxia-induced increases in *EPO* mRNA and HIF-2α protein expression were suppressed by combining SFO and cobalt chloride treatments (Figure 3E and F).

DMOG is a prolyl hydroxylase inhibitor drug, and is also used for induction of HIF expression. As observed with cobalt chloride, DMOG treatment increased *EPO* mRNA and HIF-2α protein expression, and these increases were inhibited by concomitant SFO treatment (Figure 3G and H). Cobalt- or DMOG-induced HIF-1α protein expression was also decreased by concomitant SFO treatment (Figure 3F and H).

SFO treatment induced oxidative stress

Excess iron causes oxidative stress by producing hydroxyl radicals via the Fenton reaction[29]. SFO treatment actually increased labile ferrous iron mainly in both the proximal and distal tubule of the kidney (Figure 2E and H), and HepG2 cells (Figure 4A), suggesting to iron-induced oxidative stress consequent to Fenton reaction. Here, we showed that SFO induced oxidative stress in the kidney (Figure 2F). SFO-induced oxidative stress seemed to be dominantly localized in the glomeruli and a part of the proximal tubule (Figure 2G). SFO-induced oxidative stress was also observed in HepG2 cells (Figure 4B), and it was diminished by the anti-oxidant compound, tempol (Figure 4C). Iron content was elevated with SFO-treatment, which did not change following tempol treatment (Vehicle; 424 ± 460 ng $Fe \cdot g^{-1}$protein, SFO; 9297 ± 685 ng $Fe \cdot g^{-1}$protein, SFO+tempol; 9597 ± 880 ng $Fe \cdot g^{-1}$protein). The suppressive effects of SFO on *EPO* mRNA and HIF-2α protein expression, but not *HIF-2α* mRNA, were prevented by tempol treatment (Figure 4D-F). SFO-induced reduction in HIF-1α protein was restored by tempol treatment (Figure 4F). These

findings indicate that SFO-mediated suppression of *EPO* and HIF-2α expression occurs via SFO-induced oxidative stress.

SFO suppressed the interaction between the HIF-2α protein and Epo-HRE containing promoter

We performed ChIP to examine the interaction between the HIF-2α protein and *Epo*-HRE containing promoter region. As shown in Figure 4G, SFO treatment reduced HIF-2α binding to the *Epo* promoter. The suppressive action of SFO on the HIF-2α and *Epo*-gene promoter interaction was restored by tempol treatment. These results suggest that SFO-induced *EPO* down-regulation was due to the inactivation of HIF-2α binding to the *Epo*-HRE containing promoter region.

The promoter activity of HRE was inhibited by SFO treatment in HepG2 cells

We also examined the effect of SFO on HRE promoter activity by luciferase assay. As shown in Figure 4H, SFO diminished the promoter activity of HRE by 50%, indicating the inhibitory action of SFO on *Epo* through transcriptional inactivity of HIF.

Effect of SFO on HIF-regulated genes

HIF is a well-known transcriptional regulator for many genes. In addition to *Epo*, we assessed several HIF-regulated genes, such as *Vegf, Phd3,* and *PGK1*. In the *in vivo* studies, SFO treatment elevated mRNA expression of these 3 genes (Figure 5A).

However, only *Phd3* mRNA expression was augmented by SFO treatment in HepG2 cells (Figure 5B). PHD3 plays a crucial role in the regulation of HIF-2[30], indicating the involvement of iron in HIF-2α regulation.

Inhibitory effect of SFO on anemia-induced EPO upregulation

Finally, we examined whether SFO treatment suppresses anemia-induced EPO upregulation by using mice with phlebotomy-induced anemia. Phlebotomy-induced anemia in mice, and no differences in hematological parameters were observed in these mice regardless of SFO treatment (Table 3). As shown in Figure 5C and Table 4, anemia induced an increase in renal *Epo* mRNA expression as well as plasma EPO concentration, were suppressed by SFO treatment. Moreover, anemia-induced HIF-2α expression was also inhibited in SFO-treated mice with phlebotomy (Figure 5D).

Discussion

In CKD, patients with renal anemia are commonly administered parenteral iron supplementation. However, iron treatment itself has adverse effects on various tissues through iron-related oxidative stress production. In the present study, we found that parenteral iron treatment reduced *EPO* mRNA and HIF-2α protein expression in the mouse kidney. Notably, iron treatment augmented oxidative stress production in both *in vivo* and *in vitro* experiments, and tempol could restore iron-induced reduction of *EPO* and HIF-2α expression in HepG2 cells. Moreover, iron suppressed HIF-2α

binding to the *Epo*-HRE containing promoter, which was ameliorated by tempol. These results suggest that iron reduces *EPO* expression through HIF-2α inactivation via oxidative stress production.

Renal fibrosis is an important factor in the progression of CKD leading to end-stage renal disease[31], and renal anemia, a complication of CKD, develops along with renal fibrosis. The primary cause of renal anemia is inadequate EPO production consequent to loss of renal-EPO-producing cells due to renal fibrosis[16]. The murine UUO model is widely recognized to induce renal fibrosis with reduced EPO expression. Renal EPO expression is drastically reduced at day 1 or later after UUO surgery[17]. In the same murine UUO model, excess iron accumulation is observed in UUO-induced fibrotic kidneys compared to those of sham-operated mice[15]. Additionally we confirmed reduced *EPO* expression in UUO fibrotic kidneys. Consistent with the association between renal fibrosis and iron accumulation, several studies have shown that iron content is increased in fibrotic kidneys of the angiotensin II-infused rat[32], Dahl salt-sensitive rat[33], and 5/6 nephrectomized rat[34]. We, and others, have shown the anti-fibrotic effect of tissue iron reduction using iron chelators or iron restriction chow on the kidney[15, 33, 34]. Here, direct SFO treatment diminished renal EPO expression in the kidney with increased iron content. Therefore, there is a close relationship between iron accumulation and renal fibrosis, resulting in the reduction of *EPO* expression.

The *EPO* gene promoter contains a hypoxia response element (HRE) region. HIF promotes *EPO* transcription through binding to HRE in the *Epo*-promoter[26, 35]. It has been shown that HIF-1 and HIF-2 transcriptionally regulate *EPO* expression. However, using renal specific HIF-2α knockout mice it has been demonstrated that renal *EPO* expression is predominantly regulated by HIF-2α and not by HIF-1α[36]. Using an siRNA approach in Hep3B cells, constituting a hepatoma cell line[37], and mice with conditional hepatic HIF-2α deletion it has been shown that *EPO* gene induction is largely dependent on HIF-2, not HIF-1 in the liver[26]. Thus, HIF-2α is recognized as a key regulator of *EPO* expression in both the kidney and liver.

In this study, SFO treatment reduced HIF-2α expression, and HIF-2α protein binding to the *Epo*-promoter region. Additionally, SFO-induced HIF-2α inactivation was ameliorated by the anti-oxidant compound, tempol, indicating the involvement of iron-mediated oxidative stress in HIF-2α regulation. HIFs are generally regulated by post-transcriptional mechanisms that determine the rate of HIF protein degradation[38], and its binding ability[39]. Iron itself is shown to antagonize HIF-mediated induction of *EPO* gene expression induced by cobalt chloride[40], and iron supplementation reduces HIF-1α expression levels even under normoxia in PC3 cells[41]. This is the first study to describe the association between iron and HIF-2α, and to suggest that the preventive action of iron on *EPO* expression is mediated through a HIF-2α-dependent signaling pathway. Prolyl hydroxylase domain (PHD) also plays a crucial role in regulating HIF protein stability, and PHD activity is stimulated by ferric iron, and suppressed by iron

chelation[42]. Correspondingly, DMOG, a PHD inhibitor, induced EPO expression, which was also attenuated by concomitant SFO treatment in HepG2 cells. In addition, PHD3 is known to be a regulator of HIF-2[30], and SFO increased *Phd3* mRNA expression in both the kidney and HepG2 cells, indicating the involvement of iron-induced PHD3 upregulation in HIF-2α reduction. Therefore, SFO-mediated EPO reduction might be involved in the destabilization of HIF-2α protein via the restoration of DMOG-inhibited PHD activity. In contrast to *phd3* mRNA expression, mice with SFO treatment showed increased mRNA expression of *Vegf* and *PGK*1 and these genes were not changed in HepG2 cells with SFO treatment. The different expression of HIF-regulated genes induced by iron might be due to tissue or cell from different organ.

Oxidative stress is proposed to participate in regulating the protein stability and transcriptional activity of HIF. H_2O_2 destabilizes HIFs protein under hypoxia[43, 44]. Oxidative stresses such as diamide, *N*-ethylmaleimide, and H_2O_2 also inhibit the DNA binding activity of HIF-1[39]. H_2O_2 suppresses hypoxia-induced EPO production in HepG2 cells[45], which might be due to oxidative stress-mediated HIF inactivation. Taken together, iron-induced oxidative stress could be responsible for protein stabilization and DNA binding activity of HIF. Moreover, tempol ameliorated SFO-induced inhibition of the HIF-2α–EPO signaling pathway without affecting intracellular iron content. Therefore, concomitant treatment of anti-oxidant drugs might be effective for reducing the oxidative stress induced by iron supplementation.

HIF proteins are involved in the post-transcriptional regulation of protein expression and activity as well as the regulation of mRNA transcription. Page *et al.* have shown that HIF-1α expression is increased by angiotensin II via diacylglycerol-sensitive protein kinase C-dependent transcriptional regulation in addition to the ROS-phosphatidylinositol 3-kinase pathway-dependent translational pathway[46]. A recent study has shown that mice deficient in iron-regulatory protein 1 exhibit HIF-2α protein accumulation due to de-repression of *HIF-2α* mRNA and induce renal *EPO* expression[47]. However, inconsistent with the above results, we have /HepG2 cells, indicating that iron negatively regulates *HIF-2α* expression at the transcriptional level in this study. Moreover, SFO-induced *HIF-2α* mRNA down regulation was not changed by tempol treatment, even though SFO-mediated HIF-2α protein down regulation was reversed. This suggests that iron transcriptionally regulates *HIF-2α* expression independent of iron-mediated oxidative stress, in addition to the post-transcriptional regulation of protein degradation and the DNA binding activities of HIF-2α. Further studies are necessary to clarify the mechanism of iron regulation on HIF-2α activation.

Recent studies demonstrate that renal EPO production cells are derived from fibroblasts, and the transition of fibroblast to myofibroblast is the main cause of renal fibrosis[28] and loss of EPO production in CKD[16, 17]. We previously reported that the UUO-induced increase of α-SMA expression in the interstitium was reduced by iron chelation[15]. This indicates that iron participates in the myofibroblast transition during

the process of renal fibrosis. Here, we also found that PDGF-Rβ (a fibroblast marker) and α-SMA (a myofibroblast marker) expression were enhanced, and that PDGF-Rβ and α-SMA were colocalized in the tubulointerstitium in kidneys with SFO treatment. These findings suggest that iron promotes renal fibrotic change with transition of fibroblasts to myofibroblasts, in part leading to an iron-induced reduction of *EPO* expression. In contrast, superoxide, as well as ferrous iron, was not observed in the renal tubulo-interstitium. Therefore, further studies are required to clarify the interaction between fibroblast, oxidative stress, and iron in the kidney.

In the present study, SFO-treated mice showed the reduced plasma EPO concentration and the lower level of RBC, Hb and Ht compared to vehicle-treated mice, suggesting the decrease of erythropoiesis due to iron-induced reduction of EPO production. On the other hand, WBC counts were elevated by SFO treatment. Intravenous iron treatment induces protein oxidation, which positively correlates to CRP levels in hemodialysis patients[48], indicating the association between iron-induced oxidative stress and inflammation. Therefore, iron treatment maybe causes inflammation as well as oxidative stress, resulting in the increased number of WBC.

In regard to mice model of UUO, *HIF-1α* mRNA was not changed and HIF-1α protein was diminished in UUO kidney at day 7 after surgery in our study. Souma et al. demonstrate that *HIF-1α* mRNA was increased in UUO kidney at day 2 after surgery [17]. This discrepancy of HIF-1α expression might be responsible for the

different sampling point after UUO induction or the discordance of protein and mRNA expression.

In conclusion, parenteral iron supplementation reduced *EPO* gene expression via oxidative stress-induced HIF-2α inactivation. These findings suggest a new potential risk of parenteral iron supplementation and a causative role of therapeutic excess iron in the further deterioration of endogenous erythropoietin production in CKD.

Acknowledgements

This work was partly supported by JSPS KAKENHI Grant (No. 15K01716) and the grant provided The Ichiro Kanehara Foundation to Y.I. We appreciate the excellent technical advice by Support Center for Advanced Medical Sciences, Institute of Biomedical Sciences, Tokushima University Graduate School. We would like to thank Editage (www.editage.jp) for English language editing.

Additional Information

Competing financial interests: The authors declare no competing financial interests.

Figure legends

Figure 1. Expression of erythropoietin (EPO) and hypoxia-inducible factors (HIFs) in kidneys with unilateral ureteral obstruction (UUO) and iron treatment. (A) Changes in *EPO* mRNA expression from kidney of sham-operated or UUO mice at day 7.

Quantitative real-time reverse transcriptase-polymerase chain reaction (qRT-PCR) analysis of *EPO* mRNA expression. Values are expressed as means ± SD. $^{**}P < 0.01$ vs. sham-operation. n = 12 in each group. (B) qRT-PCR analysis of HIF-2α and HIF-1α mRNA expression. Values are expressed as means ± SD. $^{**}P < 0.01$ vs. sham-operation. n = 12 in each group. (C) Right panels; representative figures of HIF-2α and HIF-1α from kidney at 7 days after sham-operation or UUO. Left panel: semi-quantitative analysis of densitometry for HIF-2α and HIF-1α expression. Values are expressed as means ± SD. $^{*}P < 0.05$, $^{**}P < 0.01$ vs. sham operation. n = 3 in each group. (D) Changes in *EPO* mRNA expression from kidney of vehicle- or SFO-treated UUO mice. qRT-PCR analysis of *EPO* mRNA expression. Values are expressed as means ± SD. $^{**}P < 0.01$ vs. vehicle. n = 11-13. (E) qRT-PCR analysis of HIF-2α and HIF-1α mRNA expression. Values are expressed as means ± SD. $^{**}P < 0.01$ vs. sham-operation. n = 11–13 in each group. (F) Left panels; representative figures of HIF-2α and HIF-1α from kidney with vehicle- or iron-treatment. Right panel: semi-quantitative analysis of densitometry for HIF-2α and HIF-1α expression. Values are expressed as means ± SD. $^{**}P < 0.01$ vs. sham operation. n = 12 in each group.

Figure 2. (A) Representative hematoxylin and eosin staining of the kidney section. (B) Western blot analysis showing induced effects of iron on PDGF-Rβ and α-SMA expression in kidney. Upper panels; representative figures of PDGF-Rβ from kidney with vehicle- or SFO-treatment. Lower panel: Semi-quantitative analysis of densitometry for PDGF-Rβ expression. Values are expressed as means ± SD. $^{*}P <$

0.05 vs. sham operation. n = 8 in each group. (C) Upper panels; representative figures of α-SMA from the kidney with vehicle- or SFO-treatment. Lower panel: semi-quantitative analysis of densitometry for α-SMA expression. Values are expressed as means ± SD. **P < 0.01 vs. sham operation. n = 4 in each group. (D) Iron-induced transition from fibroblast to myofibroblast in kidney. Representative immunohistochemistry of DAPI (blue), PDGF-Rβ (green), and α-SMA (red) staining. (E) SFO-increased labile ferrous iron in the kidney. Left panels; representative figures of RhoNox-1staining in the kidney with or without SFO treatment. Right panel: semi-quantitative analysis of fluorescence intensity. Values are expressed as means ± SD. *P < 0.05 vs. vehicle treatment. n = 4 in each group. (F) Iron-induced oxidative stress production in the kidney. Left panels; representative figures of dihydroethidium (DHE) staining in kidney with or without SFO treatment. Right panel: semi-quantitative analysis of fluorescence intensity. Values are expressed as means ± SD. **P < 0.01 vs. vehicle treatment. n = 3 in each group. (G) Fluorescence and light microscope images of DHE staining, and merged image of the same field of the kidney section. G: glomeruli. (H) Fluorescence image of lectin (green), E-cadherin (blue), RhoNOX-1 (red), and merged image of the same field of the kidney section.

Figure 3. The effect of iron on EPO and HIFs expression in HepG2 cells. (A) HepG2 cell viability was significantly decreased only by 1000 μg/ml SFO treatment. Values are expressed as means ± SD. **P < 0.01 vs. vehicle treatment. n = 8 in each group. (B) Impact of SFO on *EPO* mRNA expression and dose-dependency in HepG2 cells.

Values are expressed as means ± SD. **$P < 0.01$ vs. vehicle treatment. $n = 4$ in each group. SFO action on HIFs expression in HepG2 cells. (C) Quantitative analysis of for HIF-2α and HIF-1α mRNA expression. Values are expressed as means ± SD. *$P < 0.05$ vs. vehicle treatment. $n = 6$ (D) Upper panels; representative figures of HIF-2α, HIF-1α protein and tubulin with vehicle- or SFO treatment. Lower panel: semi-quantitative analysis of densitometry for HIF-2α protein expression. Values are expressed as means ± SD. *$P < 0.05$, **$P < 0.01$ vs. vehicle treatment. $n = 6$ in each group. (E) Impact of SFO on cobalt chloride-induced EPO, HIF-2α and HIF-1α expression in HepG2 cells. Suppressive effect of SFO on cobalt chloride-induced EPO mRNA upregulation in HepG2 cells. Values are expressed as means ± SD. *$P < 0.05$, **$P < 0.01$ vs. vehicle treatment. $n = 8$ in each group. (F) SFO suppressive action on cobalt chloride-induced upregulation of HIF-2α and HIF-1α expression in HepG2 cells. Upper panels; representative figures of HIF-2α and tubulin. Lower panel: semi-quantitative analysis of densitometry for HIF-2α expression. Values are expressed as means ± SD. *$P < 0.05$, **P < 0.01 vs. vehicle treatment. $n = 9$ in each group. Effect of SFO on DMOG-induced EPO, HIF-2α, and HIF-1α expression in HepG2 cells. (G) Inhibitive effect of SFO on DMOG-induced EPO mRNA upregulation in HepG2 cells. Values are expressed as means ± SD. *$P < 0.05$ vs. vehicle treatment. $n = 4$ in each group. (H) SFO inhibitive effect on DMOG-induced upregulation of HIF-2α and HIF-1α expression in HepG2 cells. Upper panels; representative figures of HIF-2α and tubulin. Lower panel: semi-quantitative analysis of densitometry for HIF-2α

expression. Values are expressed as means ± SD. *P < 0.05, **P < 0.01 vs. vehicle treatment. n = 8 in each group.

Figure 4. Involvement of oxidative stress in iron-induced down-regulation of EPO and HIFs expression in HepG2 cells. (A) Upper panels; representative figures of RhoNox-1 staining in HepG2 cells with or without SFO. Lower panel: quantitative analysis of fluorescence intensity measured by microplate reader. Values are expressed as means ± SD. **P < 0.01 vs. vehicle treatment. n = 8 in each group. (B) Upper panels; representative figures of DCFH-DA staining in HepG2 cells with or without SFO. Lower panel: quantitative analysis of fluorescence intensity measured by microplate reader. Values are expressed as means ± SD. *P < 0.05 vs. vehicle treatment. n = 16 in each group. (C) Effect of anti-oxidant agent on SFO-induced oxidative stress. Quantitative analysis of DCFH-DA fluorescence intensity measured by microplate reader. Values are expressed as means ± SD. **P < 0.01. n = 16 in each group. (D) Restorative effect of tempol on SFO-induced EPO mRNA down-regulation in HepG2 cells. Values are expressed as means ± SD. *P < 0.05, **P < 0.01 vs. vehicle treatment. n = 8 in each group. (E) Tempol has effect on SFO-induced HIF-2α mRNA down-regulation in HepG2 cells. Values are expressed as means ± SD. **P < 0.01 vs. vehicle treatment. n = 8 in each group. (F) Restorative effect of tempol on iron-induced down-regulation of HIF-2α and HIF-1α expression in HepG2 cells. Values are expressed as means ± SD. *P < 0.05 vs. vehicle treatment. n = 6 in each group. (G) ChIP analysis of HIF-2α protein and the *Epo* HRE containing promoter interaction in

HepG2 cells. Co-precipitated DNA fragments were detected by PCR using primers spanning the EPO HRE region. (H) SFO suppressed hypoxia-responsive element (HRE)-luciferase activity in HepG2 cells. Values are expressed as means ± SD. *P < 0.05 vs. vehicle treatment. n = 6 in each group.

Figure 5. (A) Changes in *VEGF, PHD3, and PGK1* mRNA expression in the kidney of vehicle- or SFO-treated mice. Values are expressed as means ± SD. *P < 0.05, **P < 0.01 vs. vehicle. n = 11–13 in each group. (B) The effect of SFO on *VEGF, PHD3, and PGK1* mRNA expression in HepG2 cells. Values are expressed as means ± SD. *P < 0.05 vs. vehicle. n = 4 in each group. Effects of SFO on (C) EPO and (D) HIFs in mice with phlebotomy-induced anemia. Values are expressed as means ± SD. *P < 0.05, **P < 0.01 vs. vehicle. n = 7 in each group.

References

1 Collins AJ, Foley RN, Gilbertson DT*, et al.* The state of chronic kidney disease, ESRD, and morbidity and mortality in the first year of dialysis. *Clinical journal of the American Society of Nephrology : CJASN* 2009;4 Suppl 1:S5-11.

2 Go AS, Chertow GM, Fan D*, et al.* Chronic kidney disease and the risks of death, cardiovascular events, and hospitalization. *The New England journal of medicine* 2004;351(13):1296-1305.

3 Levey AS. Controlling the epidemic of cardiovascular disease in chronic renal disease: where do we start? *American journal of kidney diseases : the official journal of the National Kidney Foundation* 1998;32(5 Suppl 3):S5-13.

4 Astor BC, Muntner P, Levin A*, et al.* Association of kidney function with anemia: the Third National Health and Nutrition Examination Survey (1988-1994). *Archives of internal medicine* 2002;162(12):1401-1408.

5 Paganini EP. Overview of anemia associated with chronic renal disease: primary and secondary mechanisms. *Seminars in nephrology* 1989;9(1 Suppl 1):3-8.

6 Kdoqi, National Kidney F. KDOQI Clinical Practice Guidelines and Clinical Practice Recommendations for Anemia in Chronic Kidney Disease. *American journal of kidney diseases : the official journal of the National Kidney Foundation* 2006;47(5 Suppl 3):S11-145.

7 Babitt JL, Lin HY. Mechanisms of anemia in CKD. *Journal of the American Society of Nephrology : JASN* 2012;23(10):1631-1634.

8 Nakanishi T, Kuragano T, Nanami M*, et al.* Importance of ferritin for optimizing anemia therapy in chronic kidney disease. *American journal of nephrology* 2010;32(5):439-446.

9 Nakanishi T, Hasuike Y, Otaki Y*, et al.* Hepcidin: another culprit for complications in patients with chronic kidney disease? *Nephrology, dialysis, transplantation : official publication of the European Dialysis and Transplant Association - European Renal Association* 2011;26(10):3092-3100.

10 Zhao N, Zhang AS, Enns CA. Iron regulation by hepcidin. *The Journal of clinical investigation* 2013;123(6):2337-2343.

11 Rooyakkers TM, Stroes ES, Kooistra MP*, et al.* Ferric saccharate induces oxygen radical stress and endothelial dysfunction in vivo. *European journal of clinical investigation* 2002;32 Suppl 1:9-16.

12 Kuo KL, Hung SC, Lee TS*, et al.* Iron sucrose accelerates early atherogenesis by increasing superoxide production and upregulating adhesion molecules in CKD. *Journal of the American Society of Nephrology : JASN* 2014;25(11):2596-2606.

13 Agarwal R, Vasavada N, Sachs NG*, et al.* Oxidative stress and renal injury with intravenous iron in patients with chronic kidney disease. *Kidney international* 2004;65(6):2279-2289.

14 Agarwal R. Proinflammatory effects of iron sucrose in chronic kidney disease. *Kidney international* 2006;69(7):1259-1263.

15 Ikeda Y, Ozono I, Tajima S*, et al.* Iron chelation by deferoxamine prevents renal interstitial fibrosis in mice with unilateral ureteral obstruction. *PloS one* 2014;9(2):e89355.

16 Asada N, Takase M, Nakamura J*, et al.* Dysfunction of fibroblasts of extrarenal origin underlies renal fibrosis and renal anemia in mice. *The Journal of clinical investigation* 2011;121(10):3981-3990.

17 Souma T, Yamazaki S, Moriguchi T*, et al.* Plasticity of renal erythropoietin-producing cells governs fibrosis. *Journal of the American Society of Nephrology : JASN* 2013;24(10):1599-1616.

18 Obara N, Suzuki N, Kim K*, et al.* Repression via the GATA box is essential for tissue-specific erythropoietin gene expression. *Blood* 2008;111(10):5223-5232.

19 Chiang CK, Tanaka T, Inagi R*, et al.* Indoxyl sulfate, a representative uremic toxin, suppresses erythropoietin production in a HIF-dependent manner. *Laboratory investigation; a journal of technical methods and pathology* 2011;91(11):1564-1571.

20 Nagai T, Yasuoka Y, Izumi Y*, et al.* Reevaluation of erythropoietin production by the nephron. *Biochemical and biophysical research communications* 2014;449(2):222-228.

21 Asai H, Hirata J, Hirano A*, et al.* Activation of aryl hydrocarbon receptor mediates suppression of hypoxia-inducible factor-dependent erythropoietin expression by indoxyl sulfate. *American journal of physiology Cell physiology* 2016;310(2):C142-150.

22 Ikeda Y, Enomoto H, Tajima S*, et al.* Dietary iron restriction inhibits progression of diabetic nephropathy in db/db mice. *American journal of physiology Renal physiology* 2013;304(7):F1028-1036.

23 Ikeda Y, Hamano H, Satoh A*, et al.* Bilirubin exerts pro-angiogenic property through Akt-eNOS-dependent pathway. *Hypertension research : official journal of the Japanese Society of Hypertension* 2015;38(11):733-740.

24 Hirayama T, Okuda T, Nagasawa H. A highly selective turn-on fluorescent probe fro iron(II) to visualize labile iron in living cells. *Chem Sci* 2013;4:1250-1256.

25 Mukaide T, Hattori Y, Misawa N*, et al.* Histological detection of catalytic ferrous iron with the selective turn-on fluorescent probe RhoNox-1 in a Fenton reaction-based rat renal carcinogenesis model. *Free radical research* 2014;48(9):990-995.

26 Rankin EB, Biju MP, Liu Q*, et al.* Hypoxia-inducible factor-2 (HIF-2) regulates hepatic erythropoietin in vivo. *The Journal of clinical investigation* 2007;117(4):1068-1077.

27 Paliege A, Rosenberger C, Bondke A*, et al.* Hypoxia-inducible factor-2alpha-expressing interstitial fibroblasts are the only renal cells that express erythropoietin under hypoxia-inducible factor stabilization. *Kidney international* 2010;77(4):312-318.

28 Kramann R, DiRocco DP, Humphreys BD. Understanding the origin, activation and regulation of matrix-producing myofibroblasts for treatment of fibrotic disease. *The Journal of pathology* 2013;231(3):273-289.

29 Kruszewski M. Labile iron pool: the main determinant of cellular response to oxidative stress. *Mutation research* 2003;531(1-2):81-92.

30 Appelhoff RJ, Tian YM, Raval RR*, et al.* Differential function of the prolyl hydroxylases PHD1, PHD2, and PHD3 in the regulation of hypoxia-inducible factor. *The Journal of biological chemistry* 2004;279(37):38458-38465.

31 Iwano M, Neilson EG. Mechanisms of tubulointerstitial fibrosis. *Current opinion in nephrology and hypertension* 2004;13(3):279-284.

32 Ishizaka N, Saito K, Furuta K*, et al.* Angiotensin II-induced regulation of the expression and localization of iron metabolism-related genes in the rat kidney. *Hypertension research : official journal of the Japanese Society of Hypertension* 2007;30(2):195-202.

33 Naito Y, Sawada H, Oboshi M*, et al.* Increased renal iron accumulation in hypertensive nephropathy of salt-loaded hypertensive rats. *PloS one* 2013;8(10):e75906.

34 Naito Y, Fujii A, Sawada H*, et al.* Association between renal iron accumulation and renal interstitial fibrosis in a rat model of chronic kidney disease. *Hypertension research : official journal of the Japanese Society of Hypertension* 2015;38(7):463-470.

35 Semenza GL, Nejfelt MK, Chi SM*, et al.* Hypoxia-inducible nuclear factors bind to an enhancer element located 3' to the human erythropoietin gene. *Proceedings of the National Academy of Sciences of the United States of America* 1991;88(13):5680-5684.

36 Kapitsinou PP, Liu Q, Unger TL*, et al.* Hepatic HIF-2 regulates erythropoietic responses to hypoxia in renal anemia. *Blood* 2010;116(16):3039-3048.

37 Warnecke C, Zaborowska Z, Kurreck J*, et al.* Differentiating the functional role of hypoxia-inducible factor (HIF)-1alpha and HIF-2alpha (EPAS-1) by the use of RNA interference: erythropoietin is a HIF-2alpha target gene in Hep3B and Kelly cells. *FASEB journal : official publication of the Federation of American Societies for Experimental Biology* 2004;18(12):1462-1464.

38 Semenza GL. HIF-1 and mechanisms of hypoxia sensing. *Current opinion in cell biology* 2001;13(2):167-171.

39 Wang GL, Jiang BH, Semenza GL. Effect of altered redox states on expression and DNA-binding activity of hypoxia-inducible factor 1. *Biochemical and biophysical research communications* 1995;212(2):550-556.

40 Ho VT, Bunn HF. Effects of transition metals on the expression of the erythropoietin gene: further evidence that the oxygen sensor is a heme protein. *Biochemical and biophysical research communications* 1996;223(1):175-180.

41 Knowles HJ, Raval RR, Harris AL*, et al.* Effect of ascorbate on the activity of hypoxia-inducible factor in cancer cells. *Cancer research* 2003;63(8):1764-1768.

42 Kaelin WG, Jr., Ratcliffe PJ. Oxygen sensing by metazoans: the central role of the HIF hydroxylase pathway. *Molecular cell* 2008;30(4):393-402.

43 Huang LE, Arany Z, Livingston DM*, et al.* Activation of hypoxia-inducible transcription factor depends primarily upon redox-sensitive stabilization of its alpha subunit. *The Journal of biological chemistry* 1996;271(50):32253-32259.

44 Wiesener MS, Turley H, Allen WE*, et al.* Induction of endothelial PAS domain protein-1 by hypoxia: characterization and comparison with hypoxia-inducible factor-1alpha. *Blood* 1998;92(7):2260-2268.

45 Fandrey J, Frede S, Jelkmann W. Role of hydrogen peroxide in hypoxia-induced erythropoietin production. *The Biochemical journal* 1994;303 (Pt 2):507-510.

46 Page EL, Robitaille GA, Pouyssegur J*, et al.* Induction of hypoxia-inducible factor-1alpha by transcriptional and translational mechanisms. *The Journal of biological chemistry* 2002;277(50):48403-48409.

47 Wilkinson N, Pantopoulos K. IRP1 regulates erythropoiesis and systemic iron homeostasis by controlling HIF2alpha mRNA translation. *Blood* 2013;122(9):1658-1668.

48 Tovbin D, Mazor D, Vorobiov M*, et al.* Induction of protein oxidation by intravenous iron in hemodialysis patients: role of inflammation. *American journal of kidney diseases : the official journal of the National Kidney Foundation* 2002;40(5):1005-1012.

Table 1 Sequence of the primers for Real-time PCR

Target gene	Forward (5′- 3’)	Reverse (5′- 3’)
mouse *EPO*	ATGTCGCCTCCAGATACCAC	CCTCTCCCGTGTACAGCTTC
mouse *HIF-2α*	CTAAGTGGCCTGTGGGTGAT	CGAAGTCCTTTGCAGACCTC
mouse *HIF-1α*	TCAAGTCAGCAACGTGGAAG	TATCGAGGCTGTGTCGACTG
mouse *VEGF*	CAGGCTGCTGTAACGATGAA	GCATTCACATCTGCTGTGCT
mouse *PHD3*	CAGGTTATGTTCGCCATGTG	TGGCGTCCCAATTCTTATTC
mouse *PGK1*	GTCGTGATGAGGGTGGACTT	TTTGATGCTTGGAACAGCAG
human *EPO*	TCCGAACAATCACTGCTGA	CCTCCCCTGTGTSCSGCTTC
human *HIF-2α*	TGCTGGATTGGTTCACACAT	GGGCCAGGTGAAAGTCTACA
human *HIF-1α*	TGCTCATCAGTTGCCACTTC	TCCTCACACGCAAATAGCTG
human *VEGF*	AAGGAGGAGGGCAGAATCAT	CACACAGGATGGCTTGAAGA
human *PHD3*	AGATCGTAGGAACCCACACG	TTCTGCCCTTTCTTCAGCAT
human *PGK1*	GAAGTGGAGAAAGCCTGTGC	GCATCTTTTCCCTTCCCTTC
36B4	GCTCCAAGCAGATGCAGCA	CCGGATGTGAGGCAGCAG

Table.2 Hematological characteristics

	RBC ($\times 10^4$/μl)	Hb (g/dl)	Ht (%)	WBC (/μl)	Platelet ($\times 10^4$/μl)
Vehicle	870 ± 50	13.2 ± 0.9	40.7 ± 2.2	4575 ± 340	58.4 ± 3.2
SFO	828 ± 54	12.6 ± 0.9	38.9 ± 2.7	7623 ± 684**	45.6 ± 7.9*

Data are means ± SD; n=4, respectively. * $P < 0.05$, ** $P < 0.01$ vs vehicle-treated mice

Table.3 Hematological characteristics

	RBC ($\times 10^4$/μl)	Hb (g/dl)	Ht (%)	WBC (/μl)	Platelet ($\times 10^4$/μl)
Control	897 ± 39	13.6 ± 0.6	40.7 ± 1.7	4367 ± 2084	54.1 ± 3.1
Phlebotomy	469 ± 87**	7.4 ± 1.3**	22.4 ± 3.6**	3766 ± 1666	54.1 ± 14.7
Phlebotomy+SFO	432 ± 14**	6.7 ± 0.4**	20.5 ± 0.3**	4600 ± 985	31.1 ± 19.2

Data are means ± SD; n=3, respectively. **$P < 0.01$ vs control mice

Table 4. Plasma EPO concentration

	Vehicle	SFO
Plasma EPO (pg/ml)	151.5 ± 44.4	103.9 ± 39.4*

Data are means ± SD; n=8-12, respectively. *$P < 0.05$ vs vehicle-treated mice

	Control	Phlebotomy	Phlebotomy +SFO
Plasma EPO (pg/ml)	148.3 ± 64.8	10731.7 ± 2366.5**	8087.5 ± 2061.3**$^{\#}$

Data are means ± SD; n=7, respectively. **$P < 0.01$ vs control mice, $^{\#}P < 0.05$ vs phlebotomy mice

Figure 1 Oshima, et al.

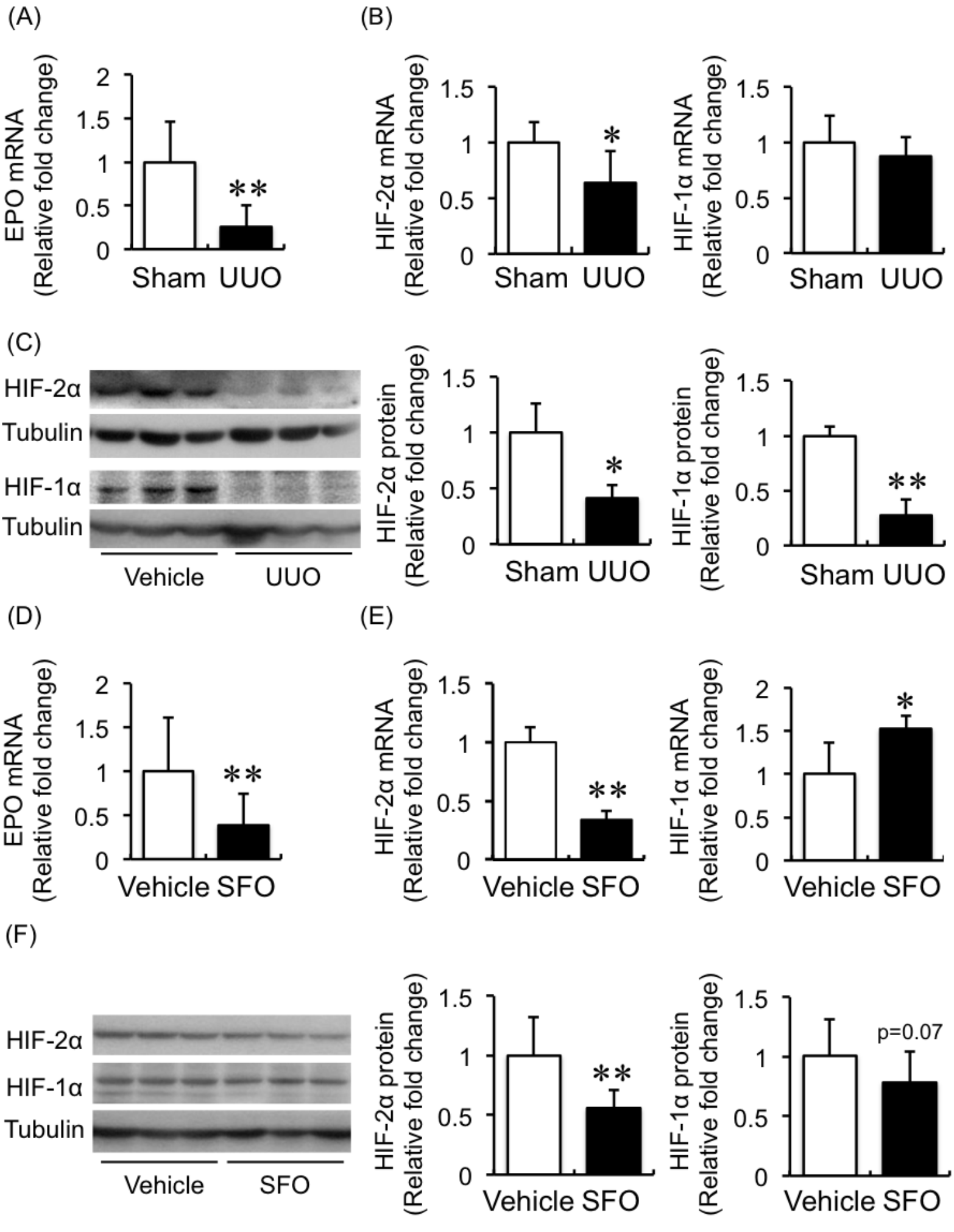

Figure 2 Oshima, et al.

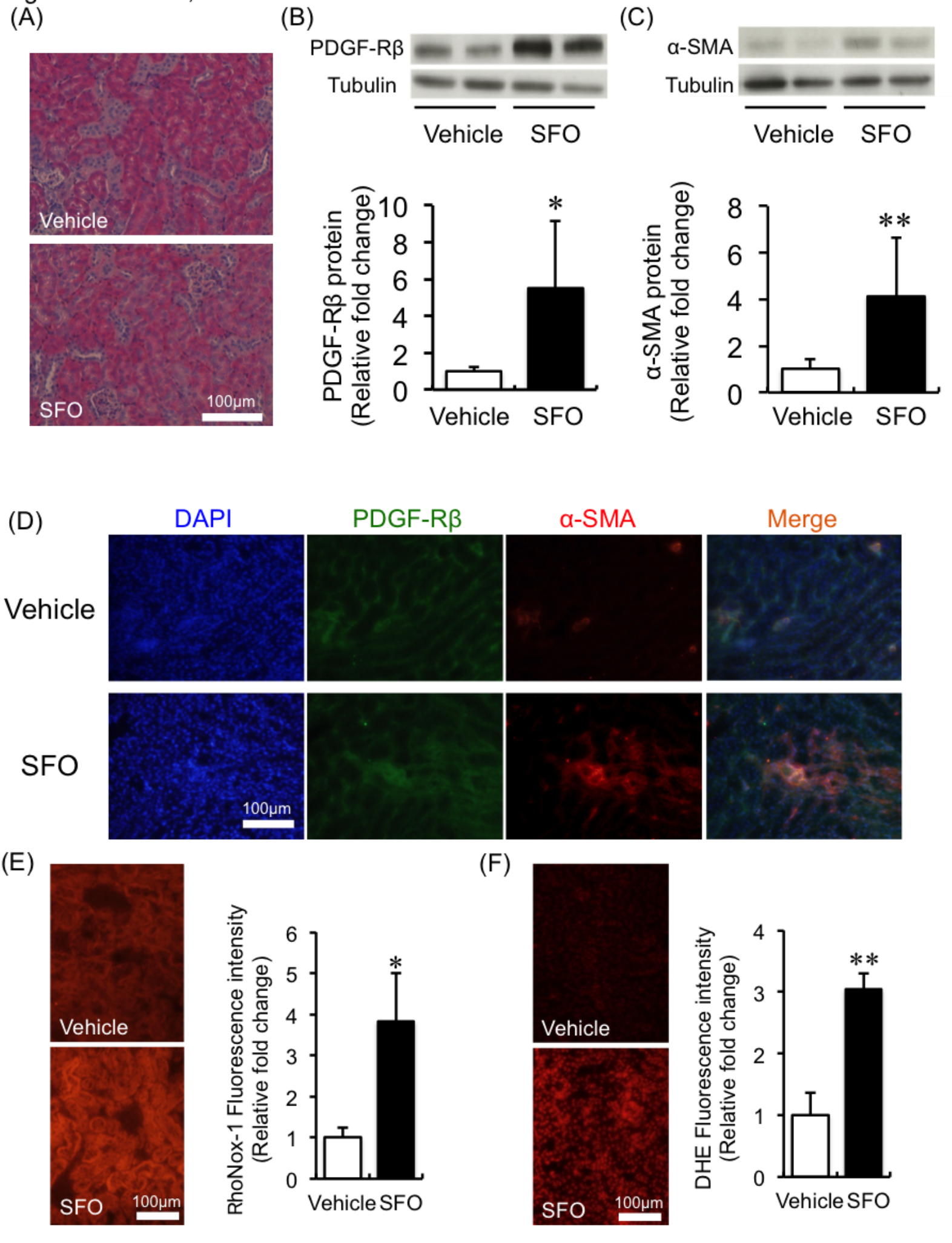

Figure 2 continued

(G)

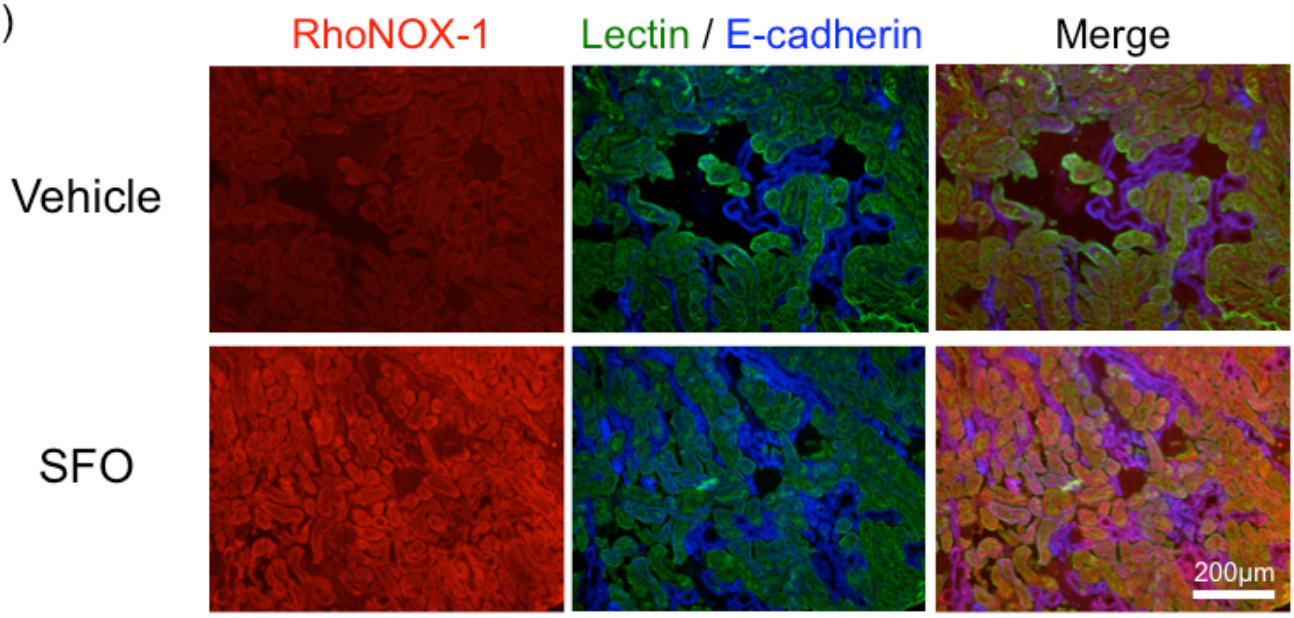

(H)

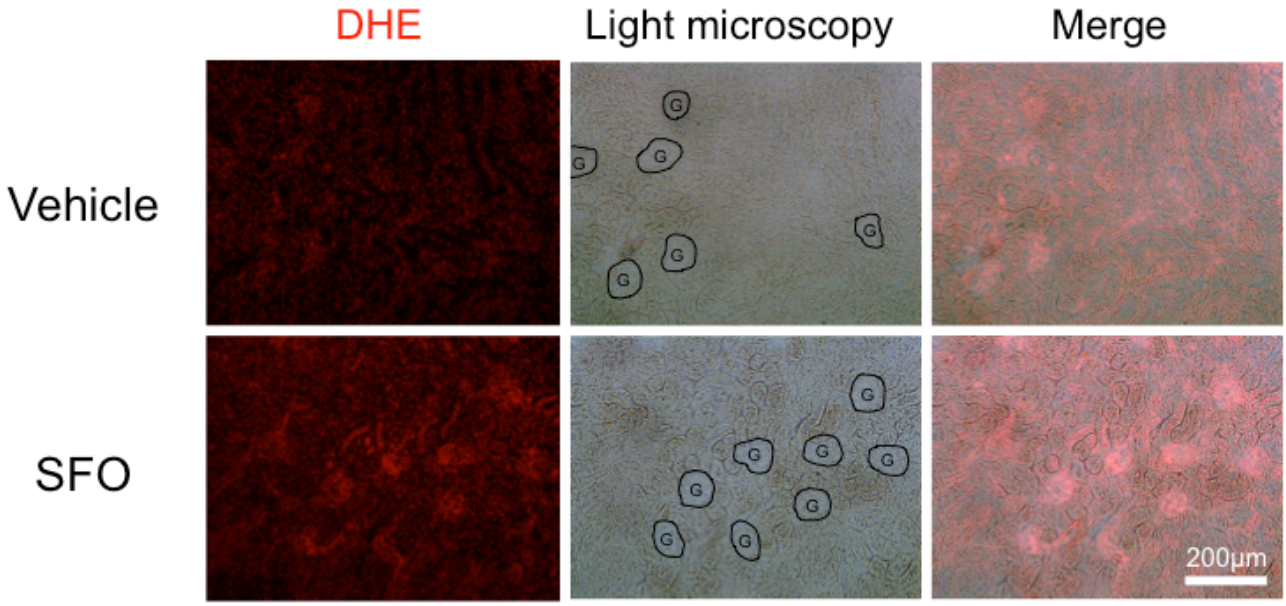

Figure 3 Oshima, et al.

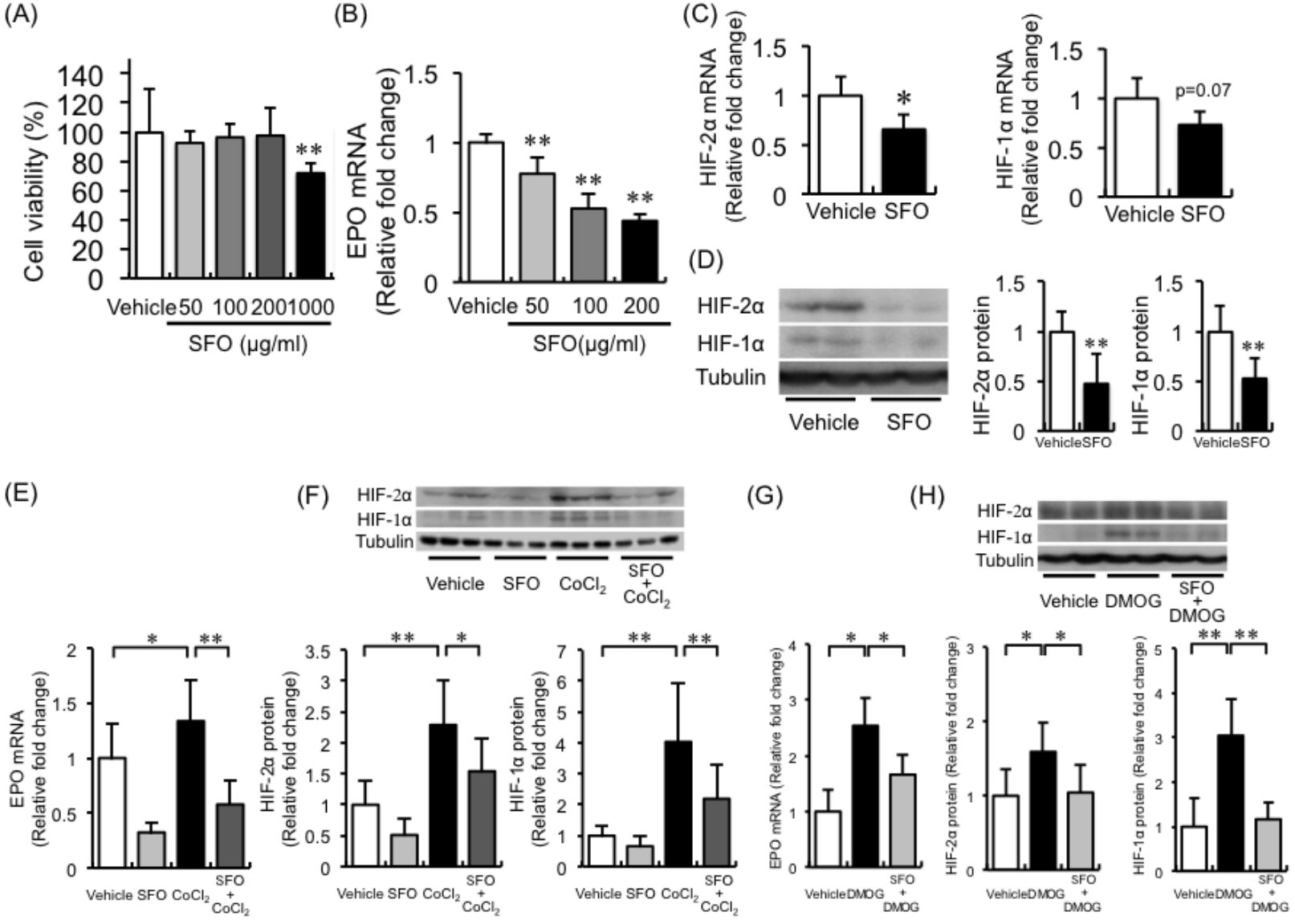

Figure 4 Oshima, et al.

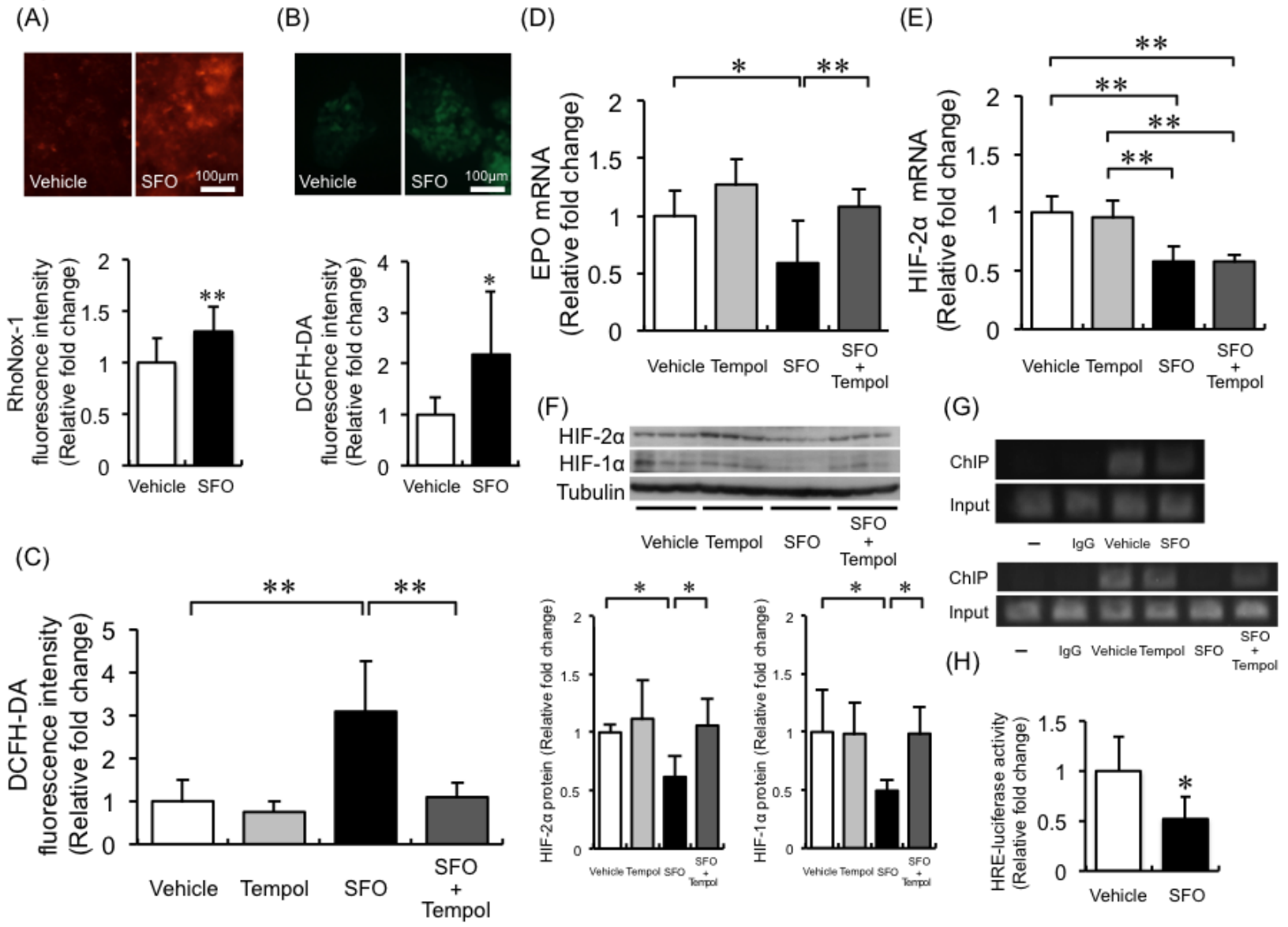

Figure 5 Oshima, et al.